PARAMETRIC STUDY OF LUNAR DUST SIMULANTS CHARGING AND TRANSPORT UNDER VUV IRRADIATION

A. Champlain(1), J.-C. Matéo-Vélez(1), J.-F. Roussel(1), S. Hess(1), P. Sarrailh(1)

(1)ONERA, The French Aerospace Lab, 2 avenue Édouard Belin, 31055 Toulouse Cedex 4, France
Email: amandine.champlain@onera.fr

ABSTRACT

Recent results of the LDEX experiment on-board the LADEE mission orbiting the Moon show that the dust particle densities at high altitude (> 10 km) are correlated with interplanetary dust impacts. This paper deals with near surface conditions (< 100 m) where electrostatic forces could also be at play. The combination of experiments and numerical simulations of dust charging under UV is used to approximate sunlit surface in the presence of craters or rocks. It is suggested that dust ejection is made possible by microscopic scale amplifications of the electrostatic forces due to soil irregularities. The importance of the dust size distribution in these effects is detailed.

1. INTRODUCTION

Lunar exploration is still an important aspect of the space agencies programs. Several projects to send equipment and/or astronauts at the surface of the Moon are in development, such as Luna-Glob Russian mission planned in 2018 with a participation of the European Space Agency (ESA). These projects justify the study of lunar dust to ensure the success of the missions since those small grains (micron to submicron diameters according to [1]) can degrade equipment by sticking on it. Recent LADEE measurements [2] have shown that dust density maps at high altitude (> 10 km) are due to interplanetary dust impacts rather than by electrostatic dust lofting. Nevertheless, the Apollo 15 and 17 missions have observed dust grains in suspension above the surface at low altitude (< 100 m), creating the Horizon Glow [3]. This dust cloud is suspected to be caused by electrostatic dust lofting due to the interaction between the grains and the environmental conditions on the Moon.

There are several charging processes happening at the lunar surface. On the dayside, the surface is mainly influenced by the photoemission current due to sunlight UV irradiation. It causes a slightly positive charge of the surface at +10 V [1, 4, 5]. On the night side, the surface is subjected to the collection of plasma particles (ions and electrons). The main electrical current is the collection of the plasma electrons, which is partly mitigated by the emission of secondary electrons from the lunar surface. Thus, the potential of the night side surface is negative and vary from -35 to -100 V according to the observations of the Lunar Prospector [1]. At the region between the sunlit and the shadowed sides, named the terminator, it has been suggested that strong electric fields are presents, due to the large variation of potentials from negative to positive values on small distances. This effect can be also found near small structures such as crates or rocks [6, 7, 8]. These amplified electric fields could be the cause of the electrostatic lofting of dust grains. In this work, we focus on dust transport in these areas.

The combination of experiments and numerical simulations is important to understand the physics of the electrostatic dust transport due to environmental conditions. A precedent work [9] detailed the first results obtained by comparing experimental tests and numerical simulations run with SPIS-Dust open-source software [8]. [9] showed the importance of the dust grain size on its ability to be electrostatically transported. Here, we focus on experiments realised in order to better understand the grain level physics at play.

Section 2 is describing the theoretical model on which the experiments are based. Section 3 presents the experimental apparatus and first results are detailed in section 4. In section 5, we discuss the perspectives of this work.

2. THEORETICAL MODEL

As exposed earlier, dust transport is enhanced at sunlit/shaded boundaries at the surface of the Moon. To better understand the dust particles dynamics, it is relevant to study the dependence of the forces acting on a dust grain as a function of its radius r_d. A grain on the lunar surface is subjected to three main forces: gravitational, cohesive and electrostatic forces. The first one is written as in [9]:

$$F_g = \frac{4}{3}\pi r_d^3 \rho g \tag{1}$$

The cohesive force is difficult to assess. Indeed, as explained in [8], it depends of a cohesion factor KS^2. This force can be written in three different ways, depending on the contact nature: two grains of the same radius, two grains with different radii and a grain on a planar surface. Respectively, the Van der Waals expressions of cohesion forces give:

$$F_c = KS^2 r_d \quad (2)$$

$$F_c = 2KS^2 \frac{r_1 r_2}{r_1 + r_2} \quad (3)$$

$$F_c = 2KS^2 r_d \quad (4)$$

The study realised in [9] showed that the value of the cohesion factor KS^2 can be restrained between 10^{-4} and 10^{-6} kg/s². To estimate more accurately this parameter, it is essential to know precisely the dust grain surface state, which is represented by the surface cleanliness S [10]. An alternative would consist in studying the effect of the dust irregular shape.

Finally, the electrostatic force depends on the grain charge Q_{grain} and the electric field applied on the particle E_{grain}. The first one is obtained by using the Gauss' theorem [8]:

$$Q_{grain} = \varepsilon_0 \pi r_d^2 E_{grain} \quad (5)$$

where ε_0 is the permittivity of free space. This force needs to take into account the effects of the dust layer topography, as shown on Fig. 1. Indeed, at microscopic scale, the geometry of the surface can cause tips effects which are amplifying each of these parameters with amplification factors β_1 and β_2 respectively. Thus, the electrostatic force is written:

$$F_e = \beta_1(\varepsilon_0 \pi r_d^2 E_{grain})\beta_2 E_{grain} \quad (6)$$

To assess the charge and the electric field at a grain level, we investigate environmental conditions near a sunlit/shade boundary by combining experiments and numerical simulations.

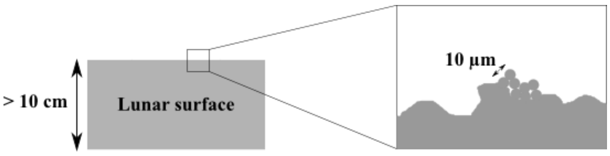

Figure 1: (left) Representation of a dust layer at a macroscopic scale. The zoomed box represents the dust layer surface at a microscopic scale, taking account of the microscopic irregularities and tips effects.

3. EXPERIMENTAL APPARATUS

In order to represent shadow/light boundaries encountered at the surface of the Moon, experiments have been conducted in the Dust Regolith or Particles (DROP) vacuum chamber at ONERA-Toulouse. It is equipped with a VUV Deuterium lamp emitting high intensity UV light with wavelengths between 115 and 400 nm**.** The illuminated zone is a circle 10 cm in diameter at the location of the test setup. A CCD camera is placed in front of one of the windows, to allow a visual diagnosis of the experiments.

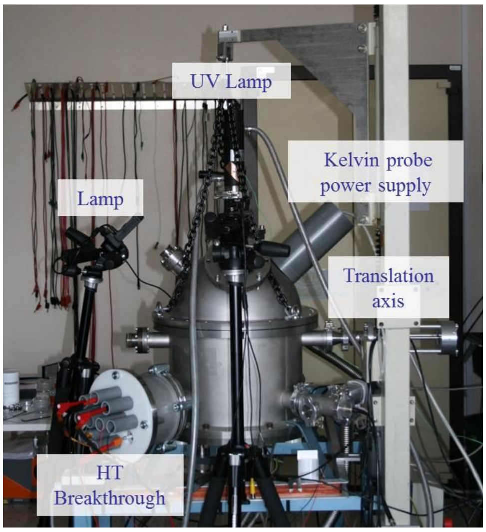

Figure 2: DROP chamber

The tests realised in this study were conducted following the geometry represented in Fig. 3, a bit different from [9]. This disposition is symmetric along the X axis and is representative of a situation where a rock shades part of the soil layer, with positive and negative surfaces close to each other. The dust layer is deposited on top of a conductive graphite support and circled with a 6mm thick Teflon plate, with a 30 mm diameter hole in it.

Two conductive blocks are placed 5 mm above the dust surface to impose an external electric field. The rectangular block at the right-hand side is conductive and it is set to a positive potential V_+ in order to attract photoelectrons emitted from the dust surface. Those photoelectrons are supposed to be efficiently hoping along the dust surface in order to charge the dust grains to a potential close to V_+. The conductive octagon on the left-hand side is mounted on a rotation axis. It allows performing eight tests instead of one for each experimental batch. Aluminum samples are vertically set on the octagon surfaces and biased to a negative potential, V_-, in order to attract the positively charged dust grains. In these experiments $V_+ = -V_-$.

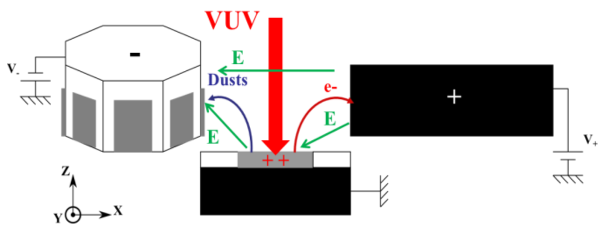

Figure 3: Experimental configuration inside DROP

Each test consists first in biasing the blocks and then in irradiating the dust during 15 min with the VUV lamp. Measurements of the dust surface potential profiles are realized with a Kelvin probe by translation along the Y axis centered on the dust surface. The assessment of dust transport is performed by in situ visual observations using a CCD camera with a resolution of 50 µm.

This experimental configuration gives electric field of about 10^5 V/m, i.e. potential variations of several thousands of volts on about ten millimeters. This is one order of magnitude larger than in experiments realized under electron beam and with dense plasma [10, 11, 12, 13, 14].

During this test campaign, the effect of the dust size distribution on the dust electrostatic transport was investigated. Four dust size distributions were tested: not sieved DNA-1 lunar dust simulant [0 – 1000 µm] and DNA-1 sieved at [0 – 25 µm], [25 – 50 µm] and [50 – 100 µm]. The observation of contaminated samples with a microscope gives pictures of the contamination. The dust size distribution on the contaminated aluminum samples is obtained by image post-processing.

4. RESULTS

Tests made with [0 – 1000 µm] distribution give a voltage threshold, at which the contamination is visible, of 3000 V. Fig. 5 shows the dust size distribution of the contamination obtained for samples biased at 3000 V and 4000 V. It seems that most of the pollution is caused by dust particles smaller than 25 µm.

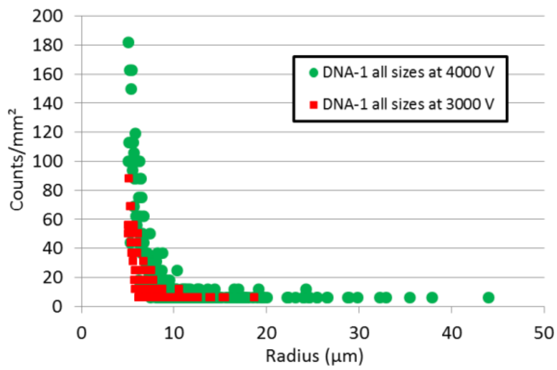

Figure 4: Dust size distributions of contamination observed at 3000 and 4000 V

Further to these observations, voltage threshold for the other size distributions were obtained as detailed in Table 1. It is noted that the [0 – 25 µm] distribution needs higher electric fields than the others, even though these grains were the main sources of contamination when using the unsieved DNA-1. Differences in electrostatic forces seem to occur.

Table 1: Voltage threshold for each dust size distribution

Dust sizes	Voltage threshold (V)
[0 – 1000 µm]	3000
[0 – 25 µm]	6000
[25 – 50 µm]	5000
[50 – 100 µm]	4000

5. PERSPECTIVES

New work will include three experimental campaigns. The first one will study the evolution of the dust layer conductivity for each dust size distribution. In a second phase, other dust materials will be submitted to the same experimental protocol. We will test the JSC-1A simulant, glass spheres of [10 – 50 µm] size distribution and DNA-1 simulant with nano-iron particles included in the silica matrix. Finally, the influence of the temperature on the voltage threshold will be investigated. These complementary tests will help us to better understand the influence of the amplification factors β_1 and β_2 and of the cohesion factor KS^2 on dust electrostatic transport.

6. REFERENCES

1. Colwell, J. E., Batiste S., Horányi M., Robertson S. & Sture S. (2007). Lunar surface: Dust dynamics and regolith mechanics, *Rev. Geophys*., 45, RG2006, doi:10.1029/2005RG000184
2. Horányi, M., Szalay J. R., Kempf S., Schmidt J., Grün E., Srama R. & Sternovsky Z. (2015). A permanent, asymmetric dust cloud around the Moon, *Nature*, 522, doi:10.1038/nature14479
3. Rennilson, J. J. & Criswell D. R. (1974). Surveyor observations of lunar horizon glow, *Moon*, 10, 121–142, doi:10.1007/BF00655715
3. Feuerbacher, B., Anderegg M., Fitton B., Laude L. D., Willis R. F. & Grard R. J. L. (1972). Photoemission from lunar surface fines and the lunar photoelectron sheath, *Proc. Third Lunar Planet. Sci. Conf*., 3, 2655–2663
4. Manka, R. H. (1973). Plasma and potentials at the lunar surface, in *Photons and Particle Interactions with Surfaces in Space*, Astrophysics and Space Science Library, vol. 37, edited by R. J. L. Grard, pp. 347–361, Springer, Netherlands
5. Criswell, D. R. (1973). Horizon-glow and the motion of lunar dust, in *Photons and Particle Interactions With Surfaces in Space*, Astrophysics and Space Science Library, vol. 37, edited by R. J. L. Grard, pp. 545–556, Springer, Netherlands
6. Poppe, A. R., Piquette M., Likhanskii A. & Horányi M. (2012). The effect of surface topography on the lunar photoelectron sheath and electrostatic dust transport, Icarus, 221, 135–146
7. Hess, S., Sarrailh P., Matéo-Vélez J.-C., Jeanty-Ruard B., Cipriani F., Forest J., Hilgers A., Honary F., Thiébault B., Marple S. R. & Rodgers D. (2015). New SPIS capabilities to simulate dust electrostatic charging, transport and contamination of lunar probes, *IEEE Transactions on Plasma Science*, Special issue for the 13th Space Charging Technology Conference
8. Champlain, A., Matéo-Vélez J.-C., Roussel J.-F., Hess S., Sarrailh P., Murat G., Chardon J.-P. & Gajan A. (2016). Lunar dust simulant charging and transport

under UV irradiation in vacuum: Experiments and numerical modeling, *J. Geophys. Res. Space Physics*, 121, 103–116, doi:10.1002/2015JA021738

9. Perko, H., Nelson J. & Sadeh W. (2001). Surface cleanliness effect on lunar soil shear strength, *J. Geotech. Geoenviron. Eng.*, 127(4), 371–383
10. Sickafoose A. A., Colwell J. E., Horányi M. & Robertson S. (2002). Experimental levitation of dust grains in a plasma sheath, *J. Geophys. Res*., 107(A11), 1408, doi:10.1029/2002JA009347
11. Flanagan T. M. & Goree, J. (2006) Dust release from surfaces exposed to plasma, *Phys. Plasma*, 13, 123504, doi:10.1063/1.2401155
12. Wang X., Horányi M. & Robertson S. (2009) Experiments on dust transport in plasma to investigate the origin of the lunar horizon glow, *J. Geophys. Res.*, 114, A05103, doi:10.1029/2008JA013983
13. Mori S., Polansky J., Masui H., Wang J. & Cho M. (2010). Development of a laboratory simulation system for lunar dust charging and levitation, paper presented at the 11th Spacecraft Charging Technology Conference, Albuquerque, New Mexico
14. Wang X., Horányi M. & Robertson S. (2010). Investigation of dust transport on the lunar surface in a laboratory plasma with an electron beam, *J. Geophys. Res.*, 115, A11102, doi:10.1029/2010JA015465